

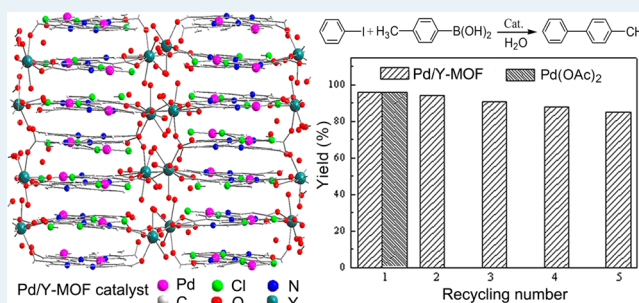
Water–Medium Organic Reactions Catalyzed by Active and Reusable Pd/Y Heterobimetal–Organic Framework

Jinping Huang,[†] Wei Wang,^{*,‡} and Hexing Li^{*,†}[†]The Education Ministry Key Lab of Resource Chemistry, Shanghai Key Laboratory of Rare Earth Functional Materials, Shanghai Normal University, Shanghai 200234, China[‡]Department of Chemistry and Chemical Biology, University of New Mexico, Albuquerque, New Mexico 87131-000

Supporting Information

ABSTRACT: A Pd/Y heterobimetallic MOF (denoted as Pd/Y-MOF) catalyst is synthesized by coordination of Pd(II) and Y(III) with 2,2'-bipyridine-5,5'-dicarboxylate (bpydc) under microwave irradiation condition and is characterized by XRD Rietveld refinement, FTIR, Raman, TG-DTA, and XPS. It is shown that the 3D extended framework is constructed by linking Pd(bpydc)Cl₂ building blocks via Y(III) coordinating to carboxylic groups. Pd/Y-MOF exhibits higher catalytic activity than Pd(bpydc)Cl₂ in Suzuki–Miyaura coupling reaction and Sonogashira reaction owing to the highly dispersed Pd(II) sites in the layered structure of Pd/Y-MOF and the cooperative effect between Pd(II) and Y(III). The heterogeneity studies provide mechanistic evidence that the reaction proceeds on the surface of Pd(II) ions in the crystal framework. Thus, Pd/Y-MOF exhibits impressive size selectivity toward substrates. With the small-sized reactants, it displays comparable activities with Pd(OAc)₂ homogeneous catalyst. However, extremely poor activity in Suzuki–Miyaura coupling reaction with bulk substrates 1-iodonaphthalene and 4-(*tert*-butyl) iodobenzene is observed due to the inhibition of diffusion into the micropore channels. In addition, Pd/Y-MOF can be easily recycled and reused owing to the high stability of the framework formed by coordination of Y(III) with carboxylic group. The incorporation of Pd(II) into the crystal framework of Pd/Y-MOF prohibits the leaching of Pd(II) active species.

KEYWORDS: Pd/Y heterobimetallic MOF (Pd/Y-MOF), heterogeneous catalyst, water–medium clean organic reactions, Suzuki–Miyaura coupling reaction, Sonogashira reaction



INTRODUCTION

Metal–organic frameworks (MOFs) represent a new class of functional materials formed by metal ions or clusters as nodes and polyfunctional organic ligands as linkers.^{1,2} The controllable topology and geometry of framework and the tunable pore functionality render them highly attractive to various applications in catalysis,^{3,4} gas storage,^{5,6} chemical separations,⁷ sensors,⁸ drug delivery,⁹ light harvesting,¹⁰ etc. With the ability to assemble well-defined molecular building blocks into microporous frameworks, MOFs are particularly suitable for immobilizing a metal complex of catalytic competence in uniform dispersion and open channel, which may display high efficiency and the advantage of easy catalyst separation from the reaction system.^{11,12} Incorporation of metal complex into a rigid lattice can effectively inhibit the leaching of active sites and also strengthen the thermal stability of the heterogeneous catalyst, leading to the enhanced catalyst durability.^{13–16} Nevertheless, to date the catalysis applications are mostly focused on the MOFs as supports for metal nanoparticles or metal complexes through postsynthesis modification.^{17,18} The direct use of MOFs catalyst is limited to MOFs only constructed by Cr(III), Zn(II), or Ln(III) ions as Lewis acid.^{19,20}

Pd(II), Rh(II), and Ru(II)-complexes catalysts are widely used in organic reaction.^{21–23} Recently, we have reported a Pd(II)-complex catalyst immobilized onto mesoporous polymer support, which can be easily recycled and repetitively used in various water-medium organic reactions.²⁴ However, it displays relatively poor activity due to the low dispersion of Pd(II) active sites and the enhanced diffusion limit resulting from the pore blockage by metal complex terminally bonded to the pore surface. It is expected that the MOFs with Pd(II) coordinated into the framework may exhibit improved activity. However, to our knowledge, no such Pd-MOF has been used in catalysis so far possibly due to the poor stability. Recently, Bordiga et al have reported the synthesis of a well-defined heterobimetallic MOFs by coordinating Pt(II) with two Cl and two N atoms in 2,2'-bipyridine-5,5'-dicarboxylate (bpydc) to form Pt(bpydc)Cl₂ building blocks, followed by linking together through Ln(III) ions bonding at carboxylic groups.^{25–28} It is noted that such heterobimetallic MOF displays strong stability, which may offer a promising way to design new Pd(II), Rh(II),

Received: February 4, 2013

Revised: May 27, 2013

Published: May 29, 2013

and Ru(II) complex catalysts in MOFs structure. The Ln(III) ions serve as cornerstones for the MOFs framework, while the noble metallic ions act as active sites for catalysis. Herein, we report for the first time the synthesis of a Pd/Y heterobimetallic organic framework (denoted as Pd/Y-MOF). Notably, it exhibits high activity in water–medium Suzuki–Miyaura coupling reaction and Sonogashira reaction.²⁸ More interestingly, it also displays size-selectivity to reactant molecules due to the diffusion limit in micropores. The catalyst can be recycled easily and used repetitively, showing great potential in practical application.

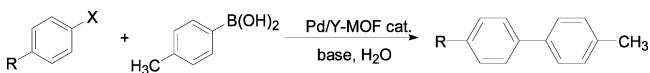
EXPERIMENTAL SECTION

1. Catalyst Synthesis. Pd/Y-MOF is synthesized under microwave irradiation conditions. In a typical synthesis, K₂PdCl₄ (0.098 g, 0.30 mmol), 2,2'-bipyridine-5,5'-dicarboxylic acid (0.073 g, 0.30 mmol) and Y(NO₃)₃·6H₂O (0.50 g, 1.3 mmol) are mixed in a Teflon-lined vessel filled with 20 mL of H₂O and stirred for 10 min at ambient temperature in air. Then, the vessel is closed in a polyether–ether–ketone (PEK) autoclave and heated rapidly to 100 °C within 1 min by microwave. The reaction system is kept at this temperature for 9 h. The resulting light yellow powder is filtered and washed thoroughly with distilled water, followed by drying in air at 80 °C. The composition of the as-received Pd/Y-MOF is determined as C₃₆H₄₀Y₂Cl₆N₆O₂₃Pd₃ based on both the ICP spectrum and elemental analysis. Experiment: C (28.3%), H (2.75), and N (5.53%). Calculation: C (26.5%), H (2.47%), and N (5.14%).

2. Characterization. Fourier transform infrared (FT-IR) spectra are collected on a Nicolet Magna 550 spectrometer. Raman spectroscopic measurement is performed by using a confocal microprobe Raman system (LabRam II, Dilor, France). Powder X-ray diffraction pattern (XRD) is recorded on a Bragg–Brentano diffractometer (Rigaku D/Max-2000) with CuKα radiation ($\lambda=1.5418$ Å) of graphite curve monochromator. The structure refinement is conducted by the GSAS suite program (the detailed procedure in the Supporting Information).²⁹ Calculation of the accessible void space to the solvent molecules is performed by PLATON program³⁰ using the as-refined crystallographic information file (CIF). In situ temperature-dependent XRD is collected in steps of 50 °C on a Buhler furnace. The sample is smeared on a platinum sample plate, allowing customized temperature programming from 50 to 900 °C with a heating ramp of 10 °C/min in air atmosphere. Thermogravimetric analysis and differential thermal analysis (TG/DTA) are conducted on a DT-60 with a heating ramp of 10 °C/min under oxygen atmosphere, respectively. The surface electronic state is analyzed by X-ray photoelectron spectroscopy (XPS, Perkin-Elmer PHI 5000C ESCA). All the binding energy values are calibrated by using C_{1s} = 284.6 eV as a reference. The content of Pd, Y and C, H, N are determined by inductively coupled plasma optical emission spectra (ICP, Varian VISTA-MPX) and elemental analysis (Elementar Vario EL), respectively.

3. Activity Test. Suzuki–Miyaura Coupling Reaction. As shown in Scheme 1, an aryl halide (0.50 mmol),

Scheme 1. Pd/Y-MOF-Catalyzed Suzuki–Miyaura Reaction

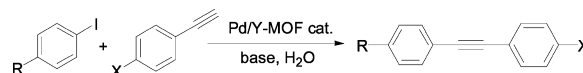


methylphenylboronic acid (0.75 mmol), K₂CO₃ (1.5 mmol), Pd/Y-MOF catalyst (0.018 mmol) containing Pd (0.054 mmol),

and 4.0 mL of H₂O are mixed and reacted at 80 °C for a specified time under mild stirring. Then, the reaction system is extracted with ethyl acetate and analyzed on a GC-17A gas chromatograph (SHIMADZU) equipped with a JWDB-5, 95% dimethyl-5% diphenylpolysiloxane column, and an FID detector. The column temperature is programmed from 80 to 250 °C at a speed of 10 °C/min. N₂ is used as carrier gas, and *n*-decane is used as an internal standard. The reaction conversion is calculated based on aryl halide since the other reactant methylphenylboronic acid is in great excess. Besides the target product biphenyl, no significant side product is observed via GC, showing the reaction is quite selective. The selectivity toward target product is further detected based on the ratio of the real biphenyl amount determined by GC using commercial available biphenyl as a standard to the theoretical biphenyl amount calculated from the conversion, which shows more than 99.5% selectivity by using chloro-, bromo-, and iodobenzene as the reactant, implying that, as observed elsewhere,^{31,32} Suzuki–Miyaura coupling reaction may proceed almost absolutely selective to the target product in most cases, that is, the yield is equal to the conversion.

Sonogashira Coupling Reaction. As shown in Scheme 2, an aryl halide (0.50 mmol), phenylacetylene (0.60 mmol),

Scheme 2. Pd/Y-MOF-Catalyzed Sonogashira Reaction



1,8-diazabicyclo[5.4.0]undec-7-ene (DBU, 0.10 mL), *n*-decane (0.10 mL), Pd/Y-MOF catalyst (0.018 mmol) containing Pd (0.054 mmol), and 4.0 mL of H₂O are mixed and reacted at 90 °C under air.

4. Adsorption Test. The adsorption performance of Pd/Y-MOF catalyst is tested in the following procedure: 2.0 mL of ethyl acetate containing a substrate (0.050 mmol) is mixed with the Pd/Y-MOF catalyst containing Pd (0.054 mmol), followed by stirring at room temperature. The content of the substrate in the solution at different time is analyzed by a gas chromatograph (SHIMADZU GC-17A) as described above.

5. Recycling Test. To determine the durability and recyclability, the catalyst is allowed to centrifuge after each run of reaction and the clear supernatant liquid is decanted slowly. The catalyst is washed thoroughly with deionized water and ethanol, followed by vacuum drying at 80 °C overnight. Then, the catalyst is reused with fresh charge of reactant for subsequent recycle under the identical reaction condition. The reproducibility of each activity test is checked by repeating each result at least three times and is found to be within acceptable limit ($\pm 5\%$).

RESULTS AND DISCUSSION

1. Structural Characterization. The XRD pattern in Figure 1 displays a long-range crystalline structure in which all diffraction peaks coincide with the reported Pt/Y-MOF.²⁵ No significant diffraction peak of impurity or start material is observed, suggesting the formation of unique phase of Pd/Y-MOF, isostructural Pt/Y-MOF in *orthorhombic*, *Pbca* (*No.* 61) space group. Therefore, the crystal structure refinement of Pd/Y-MOF is conducted by the GSAS suite²⁹ using atomic parameters of Pt/Y-MOF as an initial model (see Support Information for the refinement details). The final fitting factors of Sig = 1.147, $R_w = 5.626\%$, $R_{wnb} = 5.280\%$, $R_b = 3.943\%$, and

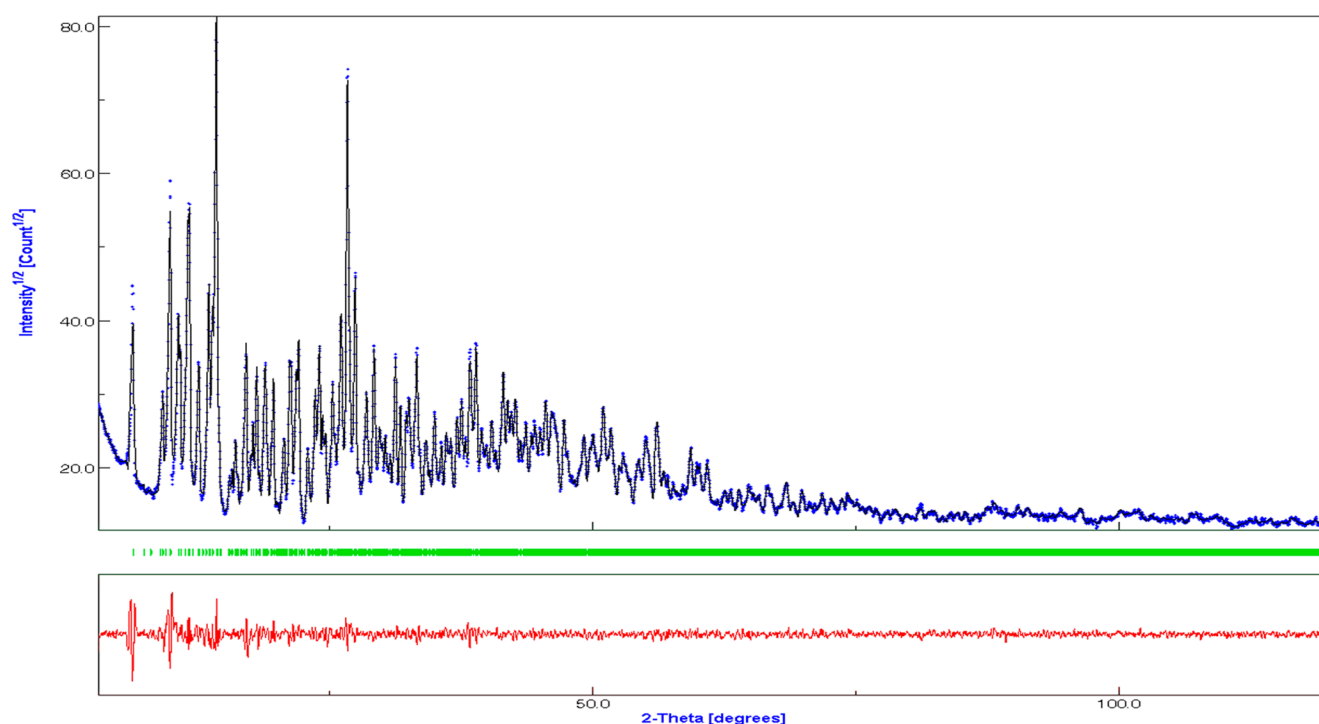


Figure 1. Rietveld refinement of XRD patterns for Pd/Y-MOF. The observed counts and the calculated patterns are indicated by blue dots and black line. The positions of Bragg reflections are indicated by vertical bars in green and the difference between observed and calculated patterns are shown by red line.

Table 1. Structural and Crystallographic Parameters of Pd/Y-MOF

		unit cell dimensions	
Pd/Y-MOF formula	$H_{40}C_{36}Cl_6N_6O_{23}Pd_3Y_2$	<i>a</i> (Å)	18.0492(1)
formula weight	1634.6	<i>b</i> (Å)	20.0984(5)
crystal system	orthorhombic	<i>c</i> (Å)	28.2613(1)
space group	<i>Pbca</i> (No. 61)	<i>Z</i>	8

$R_{\text{exp}} = 4.906\%$ represent a satisfactory refinement result. The crystallographic parameters of Pd/Y-MOF are listed in Table 1.

As illustrated in Figure 2, each of the three crystallographically nonequivalent Pd atoms constructs a square planar coordination mode connecting two N-atoms in a bpydc molecule and two Cl-atoms in the remaining cis-positions with the average bond distances of $d_{\text{Pd-N}} = 2.02(1)$ Å and $d(\text{Pd-Cl}) = 2.30(2)$ Å, respectively. The N–Pd–N angle in Pd/Y-MOF severely contracts from normal 90° to around 80.3° . Correspondingly, the Cl–Pd–N angle expands from normal 90° to about 95.6° , indicating a typical mode of cis-chelating bipyridine. Raman spectra (Supporting Information Figure S2) display two peaks for Pd–Cl stretching at 350 and 309 cm^{-1} indicative of the cis-geometry for $[\text{PdLCl}_2]$ complex.³³

Two crystallographically independent Y atoms with similar coordination environment form into Y dimers with $d(\text{Y1-Y2}) = 5.439(3)$ Å. Each Y atom coordinates with eight O-atoms, five of which are from the carboxyl in four different bpydc in $(\text{bpydc})\text{PdCl}_2$ primary units with $d(\text{Y-O})$ around 2.24–2.49 Å. Except one bridged chelating bidentate coordination, the other carboxylic groups are coordinated to Y ion in monodentate mode. The crystallographically nonequivalent Y unit also contains three coordinated water molecules with $d(\text{Y-OW})$ around 2.33–2.44 Å. These Y dimers are located separately with distance around 11 Å in [010] direction, creating cages containing residual

free water molecules. Calculation by PLATON program³⁰ gives 16.8% accessible void space to the solvent molecules. This value is low comparative to most MOFs materials. However, S. Bordiga et al.²⁵ have demonstrated that the internal void of the Pt/Y-organic framework is accessible to water, methanol, ethanol, and acetonitrile. The main bond distances and angles are listed in Table 2.

The crystal structure of Pd/Y-MOF is constructed by sheets stacking along [010] direction with the space between layers around 3.3 Å (Figure 3). These sheets are formed by packing the primary unit of $\text{Pd}(\text{bpydc})\text{Cl}_2$ in a zigzag along [100] direction in which each sheet rotates by 47° . The Pd(II) ions are uniformly distributed along [100] direction with the distance between two neighboring Pd atoms around $9.6051(7)$ Å. Every two Y dimers connects three successive sheets of $\text{Pd}(\text{bpydc})\text{Cl}_2$ through coordination of Y ions with O atoms of carboxylic groups in bpydc and water molecules, leading to the formation of well-defined MOF framework.

Figure 4 shows the TG-DTA curves and in situ XRD patterns of Pd/Y-MOF in air atmosphere. The first weight-loss of 4.9% related to the endothermic process around 150°C can be assigned to the removal of adsorbed water or organic solvents. Correspondingly, no significant structure transformation is observed in XRD pattern and Pd/Y-MOF well retained its original structure up to 500°C . Around 500°C , a strong exothermic peak occurs, corresponding to the weight loss of 65% because of the combustion of bpydc ligand. This amount is in good accordance with the calculated value of bpydc (67%). The XRD patterns also reveal the formation of Y_2O_3 (PDF 41-1105) and metallic Pd (PDF 46-1043) phases after 500°C . Further increasing temperature above 500°C , PdO (PDF 43-1024) appears.

The XPS spectra of Pd/Y-MOF, $\text{Pd}(\text{bpydc})\text{Cl}_2$ and $\text{Y}(\text{CH}_3\text{COO})_3$ are illustrated in Figure 5. All the Pd species in Pd/Y-MOF are present in +2 oxidation state, corresponding to binding energy (BE) of 337.7 and 342.9 eV of $\text{Pd}_{3d_{5/2}}$ and

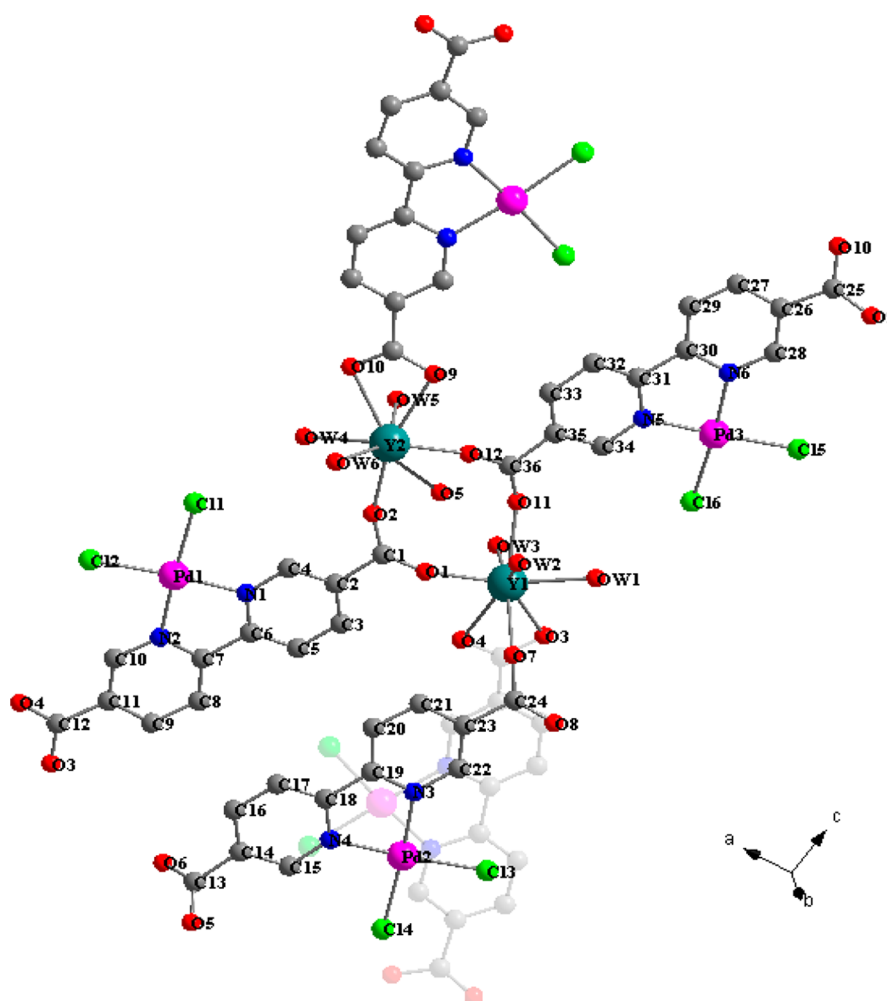


Figure 2. Pd and Y coordination environments.

Table 2. Selected Bonding Distances and Angles of Pd- and Y-Coordination Atoms in Pd/Y-MOF

bonding distance (Å)		bonding angle (degree)			
Pd1–N1	2.0171(1)	Y1–O1	2.2429(2)	N1–Pd1–N2	80.675(4)
Pd1–N2	2.0111(1)	Y1–O3	2.4907(1)	N1–Pd1–Cl1	95.536(4)
Pd1–Cl1	2.3005(1)	Y1–O4	2.4347(1)	N1–Pd1–Cl2	176.238(5)
Pd1–Cl2	2.3061(2)	Y1–O7	2.3365(1)	N2–Pd1–Cl1	175.079(6)
Pd1–Cl3	2.3005(1)	Y1–O11	2.3044(1)	N2–Pd1–Cl2	95.574(4)
Pd2–N3	2.0314(1)	Y1–OW1	2.3382(1)	Cl1–Pd1–Cl2	88.225(4)
Pd2–N4	2.0148(1)	Y1–OW2	2.395(1)	Cl3–Pd2–Cl4	88.562(4)
Pd2–Cl3	2.2964(2)	Y1–OW3	2.393(1)	N3–Pd2–Cl3	95.921(4)
Pd2–Cl4	2.3066(1)	Y2–O2	2.2176(1)	N3–Pd2–Cl4	174.836(6)
Pd3–N5	2.0238(1)	Y2–O5	2.3314(1)	N4–Pd2–N3	80.056(4)
Pd3–N6	2.0194(1)	Y2–O9	2.4424(1)	N4–Pd2–Cl3	175.498(5)
Pd3–Cl5	2.3096(1)	Y2–O10	2.4694(1)	N4–Pd2–Cl4	95.370(4)
Pd3–Cl6	2.3014(1)	Y2–O12	2.2565(2)	N5–Pd3–Cl5	174.879(5)
		Y2–OW4	2.4391(1)	N5–Pd3–Cl6	174.879(5)
		Y2–OW5	2.376(1)	N6–Pd3–N5	80.140(4)
		Y2–OW6	2.3622(1)	N6–Pd3–Cl5	95.792(4)
				N6–Pd3–Cl6	175.461(6)
				Cl5–Pd3–Cl6	88.383(4)

$\text{Pd}_{3d_{3/2}}$ level, respectively.³⁴ Compared with $\text{Pd}(\text{bpydc})\text{Cl}_2$, the Pd (II) BE in Pd/Y-MOF shifts negatively by 0.2 eV, suggesting that the N atom donates partial electrons to Pd (II) and a stronger coordination of Pd (II) with the N atoms on pyridine

ring in Pd/Y-MOF than that in $\text{Pd}(\text{bpydc})\text{Cl}_2$. A possible reason is the formation of Y–O coordination bond in which the O of carboxyl group gives partial electrons to Y(III). The decreasing electron density around O atoms result in the increasing of electron density around the N atom in bipyridine ring, leading to the N atom further donate electrons to Pd (II).³⁴ This is confirmed by the positive BE shift of O and the negative shift of N in Pd/Y-MOF comparing to those in $\text{Pd}(\text{bpydc})\text{Cl}_2$. All Y–O bonding lengths in Pd/Y-MOF are generally shorter than that in $\text{Y}(\text{CH}_3\text{COO})_3$ (2.33 Å, CSD CIF CEBFUL01), implying the stronger Y–O interaction in Pd/Y-MOF (Table 2). The negative BE shift of Cl can also be explained in the similar way. Meanwhile, FT-IR spectra (Supporting Information Figure S1) shows that in comparison with the free bpydc, the Pd/Y-MOF has no significant absorption bands of $\nu(\text{C}=\text{O})$ at 1649 and 1258 and the bands at 2510–3020 cm^{-1} , which indicates a complete deprotonation of carboxyl acid molecules and also confirms the coordination between Y(III) ion and bpydc ligand.³⁵ The blue shift of the absorbance bands in Raman spectra at 1446 and 1329 cm^{-1} characterized by bipyridine molecule further provides the evidence of the coordination between Pd (II) ion and bpydc through the N atom in bipyridine ring.³³

2. Catalyst Performance. A series of aryl halides and 4-methylphenylboronic acid are employed as reactants in Suzuki–Miyaura coupling reaction to evaluate the catalytic performance of Pd/Y-MOF. As shown in Table 3, the catalytic

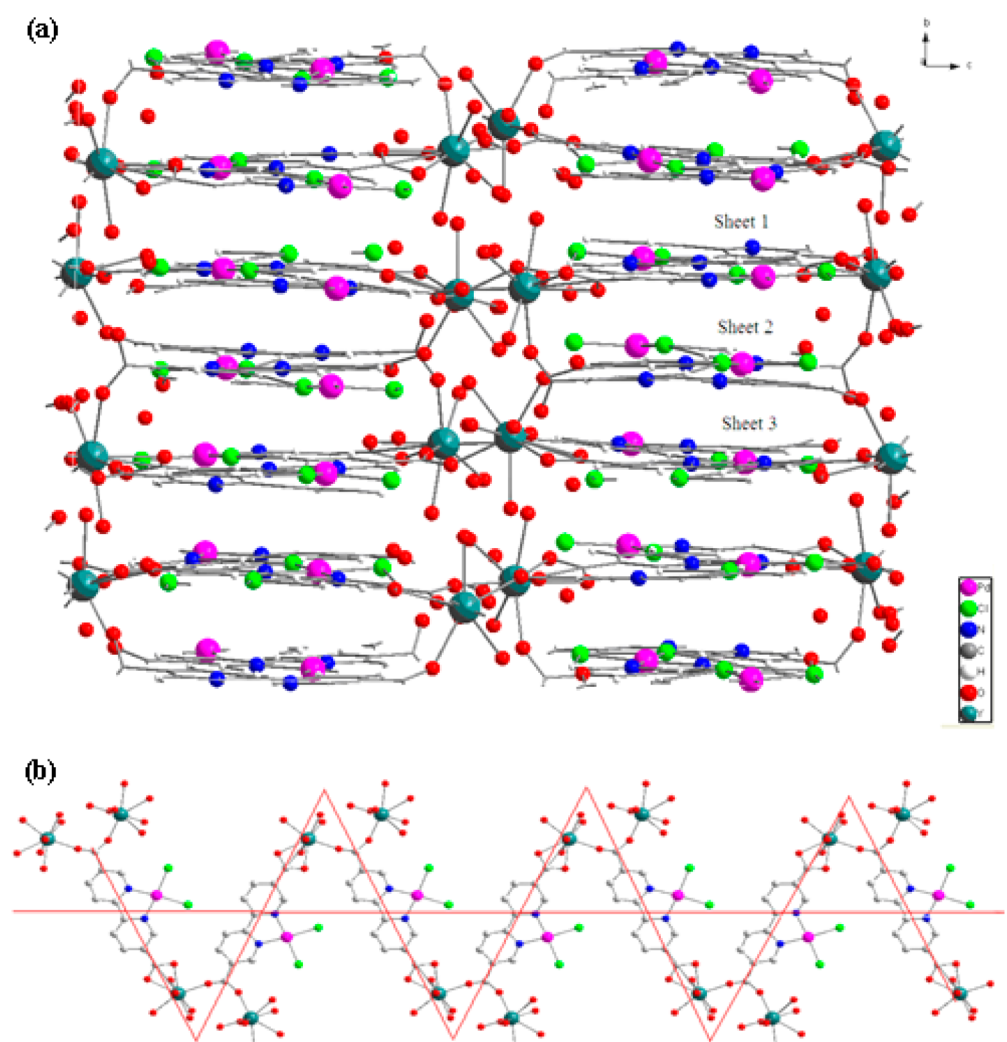


Figure 3. Crystal structure of (a) Pd/Y-MOF view along [100] and (b) the units of Pd(bpydc)Cl₂ building blocks packed in a zigzag along [100].

activity decreases from iodobenzene to bromobenzene to chlorobenzene because of the enhanced difficulty for activating the C-halide bond. Suzuki–Miyaura coupling reaction between chlorobenzene and 4-methylphenylboronic acid displays very low conversion (22%) even after the reaction for 12 h (4 h more than other reactions) in the presence of tetrabutylammonium bromide (TBAB). The presence of CH₃- and CH₃O-groups on the iodobenzene slightly suppresses the reaction activity. Similar result is also observed by using Pd(OAc)₂ homogeneous catalyst, suggesting that the electron-donating substitutes may stabilize the C-halides bond against activation, leading to the poor activity. On the other hand, the presence of electron-withdrawing substitute group (–NO₂) on the iodobenzene greatly promotes the reaction and the conversion reaches 96% even after reaction for 6 h. It is also found that Pd/Y-MOF shows much higher activity than the Pd(bpydc)Cl₂ solid catalyst, possibly owing to the exposed Pd(II) sites in the layered structure constructed by linking the Pd(bpydc)Cl₂ building blocks through Y(III) coordinating with carboxylic groups (see Figure 3). Meanwhile, as above-mentioned, the coordination of Y(III) and carboxylic groups results in N further donating electron to Pd (II) (Figure 5). The corresponding increase in electron density on Pd (II) may facilitate the initial adsorption and insertion of aryl halides molecules to Pd active sites

according to common mechanism of Pd-catalyzed carbon–carbon coupling reaction.^{36–38}

Pd/Y-MOF shows the same catalytic activity as the Pd(OAc)₂ homogeneous catalyst in Suzuki–Miyaura coupling reaction between 4-methylphenylboronic acid and iodobenzene, obviously owing to the extremely high dispersed Pd (II) active sites and the low diffusion limit. The activity difference between Pd/Y-MOF and Pd(OAc)₂ presents in bulky aryl halide substrate, which can be attributed to the enhanced diffusion limit of reactant molecule in the micropore channel. It is noted that using iodobenzene and 1-iodonaphthalene as reactant, Pd/Y-MOF catalyst affords the discrepant conversion up to 50%, which is comparative to that of NaX zeolite-supported Pd (II) catalyst,³⁹ taking into account that the micropore size of the Pd/Y-MOF framework is only about 3.3 Å (see Figure 3). When 4-(*tert*-butyl) iodobenzene bearing a very large *t*-bu group is used in the reaction, the Pd/Y-MOF exhibits extremely low activity because of both the inhibition of reactant molecules into micropore channels and electron effect. In contrast, the Pd(OAc)₂ homogeneous catalyst still shows relatively high activity for both small and bulk substrates owing to the absence of diffusion limit.

We have attempted to evaluate the microporosity and surface area of the Pd/Y-MOF material by the classical N₂ adsorption at 77 K. The obtained adsorption capacity is as low as

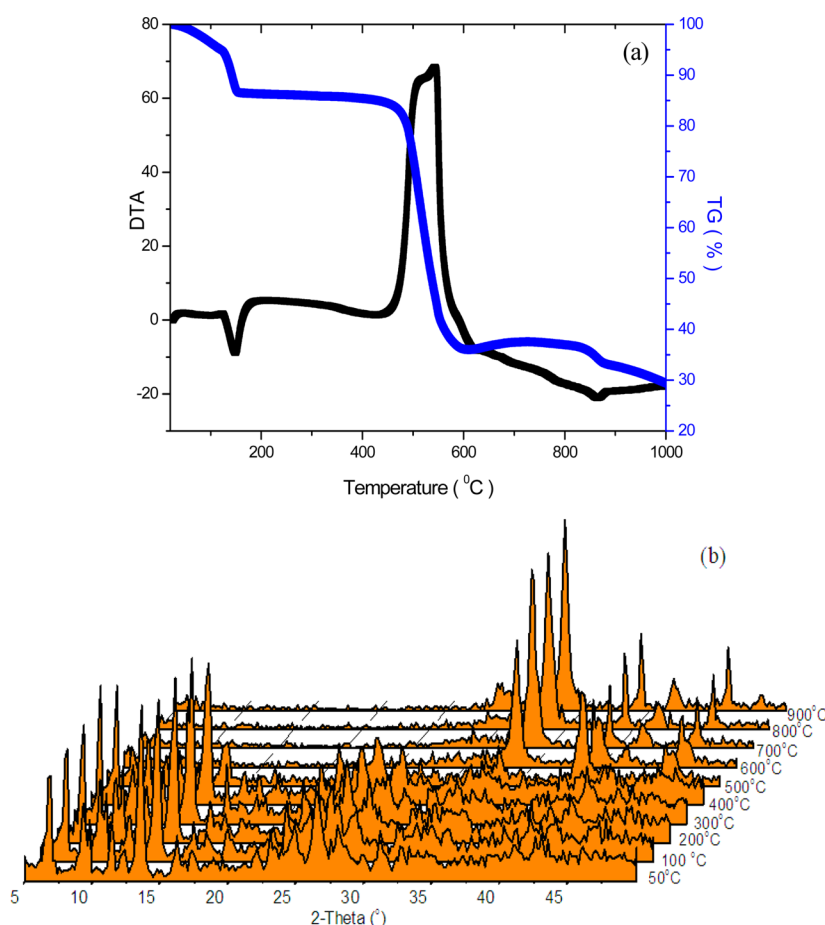


Figure 4. TG-DTA curves (a) and in situ variable-temperature XRD patterns (b) of Pd/Y-MOF.

Pt/Y-MOF reported by S. Bordiga,²⁵ which is ascribed to nonpolar N₂ can only perform weak intramolecular interaction with the lattice and cannot create the swelling of the pores that the molecular penetrate inside the MOF needed. As a consequence, the surface area measured via N₂ adsorption only probes the external surface. To understand the great difference in Suzuki–Miyaura coupling reaction efficiencies with iodobenzene, 1-iodonaphthalene, and 4-(*tert*-butyl)iodobenzene as substrates, their adsorption performances on the Pd/Y-MOF catalyst are examined, respectively. As shown in Figure 6, the Pd/Y-MOF catalyst displays more rapid adsorption to iodobenzene than to 1-iodonaphthalene and 4-(*tert*-butyl)iodobenzene, obviously owing to the lower diffusion limit. Meanwhile, Pd/Y-MOF catalyst exhibits much higher adsorption capacity for iodobenzene than for 1-iodonaphthalene and 4-(*tert*-butyl)iodobenzene, because the large molecule size of adsorbates needs more space of the micropores of Pd/Y-MOF catalyst and also blocks the pore entrance, leading to the rapid stop of the adsorption for 1-iodonaphthalene and 4-(*tert*-butyl)iodobenzene. These results clearly demonstrate that the diffusion of the reactant molecule in the micropores of the Pd/Y-MOF catalyst plays a crucial role in determining the catalytic activity and selectivity. In other words, the reactants and products in these reactions have to be sufficiently small so that the reaction can take place inside the micropores of Pd/Y-MOF (diameter ≈ 3.3 Å). Similar results are also observed in the Sonogashira coupling reaction. As shown in Table 4, Pd/Y-MOF catalyst also shows much higher activity than that of the Pd(bpydc)Cl₂ owing to the cooperative effect between Y(III) and Pd(II) in

Pd/Y-MOF network. Meanwhile, a similar trend is observed for the decreased activity in sequence of $-H$, $-CH_3O$, $-CH_3$, and $-C(CH_3)_3$ on iodobenzene, which further confirms that enhanced diffusion limit of the reactant with bulk molecule and the electronic effect. The presence of electron-withdrawing group ($-NO_2$) on iodobenzene promoted the reaction activity due to the activation of C–I bond. It is interesting to find that CH_3O -substituted group on iodobenzene and phenylacetylene plays a contrary role in the Sonogashira coupling reaction catalyzed by Pd/Y-MOF. The presence of CH_3O -group on the phenylacetylene promotes rather than hampers reaction possibly owing to the activation of the $C\equiv C$ triple bond by an electron-donating group.

3. Heterogeneity Test. As shown in Figure 7, Pd/Y-MOF catalyst can be used repetitively in Suzuki–Miyaura coupling reaction between iodobenzene and 4-methylphenylboronic acid for more than 5 times without significant decrease in activity. Similarly, it also shows good durability in the Sonogashira coupling reaction between iodobenzene and phenylacetylene. The XRD patterns (Supporting Information Figure S3) reveal that the Pd/Y-MOF catalyst retains its original crystalline structure well after being used repetitively for three times. The change of the relative intensities of some diffraction peaks may result from the micropores blockage from the solvent, showing excellent hydrothermal stability of the MOF framework. The stabilizing effect of the Y(III) coordinated with carboxyl of bpydc is essential to reserve the chemical microenvironment of the Pd(II) active sites. Meanwhile, the ICP analysis demonstrates that the leaching of Pd(II) species from the Pd/Y-MOF

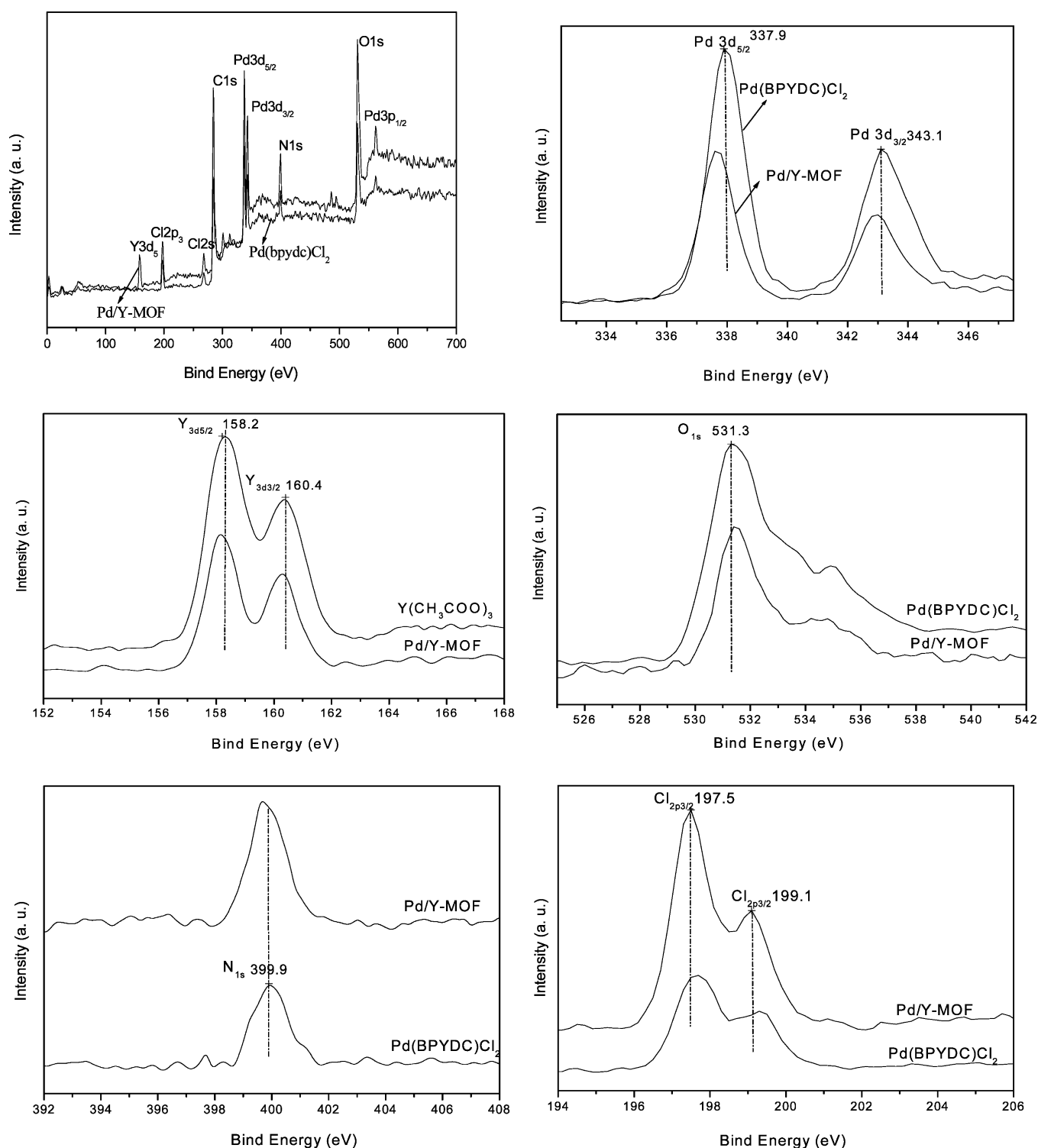
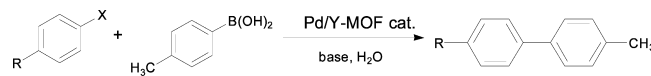


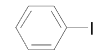
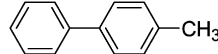
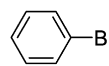
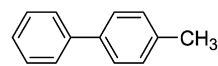
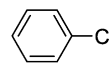
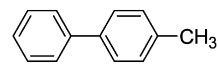
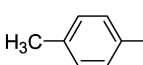
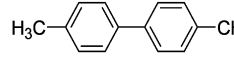
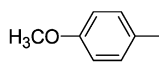
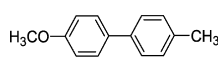
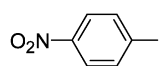
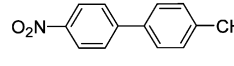
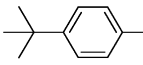
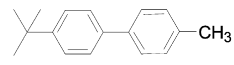
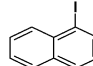
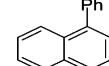
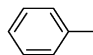
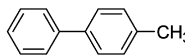
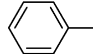
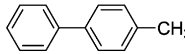
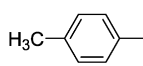
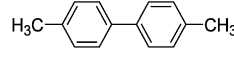
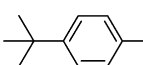
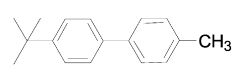
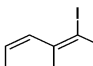
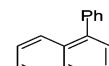
Figure 5. XPS spectra of Pd/Y-MOF, Pd(bpydc)Cl₂, and Y(CH₃COO)₃.

catalyst is neglected during the successive reactions because the Pd (II) ions are incorporated into the MOF framework via coordination. The slight decrease in the activity in each subsequent reaction can be attributed to the loss of trace Pd/Y-MOF catalyst during its separation and washing process from the reaction system.

The nature of the active Pd species (homogeneous vs heterogeneous) in C–C coupling reaction has been a matter of much debate.^{28,40,41} To make sure whether the Pd (II) active sites

incorporated into the Pd/Y-MOF framework or the homogeneous Pd (II) species leached from the solid catalyst during reaction are truly catalyst, a series of tests including hot filtration, solid-phase poisoning test^{42–45} and three-phase test.^{46–48} are carried out (for the detailed procedure, see Support Information). The present Pd/Y-MOF catalyst seems to catalyze the coupling reactions in a truly heterogeneous manner. This conclusion is based on the following observations. (1) During the reaction, we remove the Pd/Y-MOF by

Table 3. Suzuki–Miyaura Coupling Reactions between Aryl Halides with 4-Methylphenylboronic acid^a


Catalyst	Aryl halide	Reaction time (h)	Product	Yields (%)
Pd/Y-MOF		8		96
Pd/Y-MOF		8		59
Pd/Y-MOF		12		22
Pd/Y-MOF		8		86
Pd/Y-MOF		8		88
Pd/Y-MOF		6		96
Pd/Y-MOF		8		5.5
Pd/Y-MOF		8		46
Pd(bpydc)Cl ₂		8		65
Pd(OAc) ₂		8		96
Pd(OAc) ₂		8		92
Pd(OAc) ₂		8		79
Pd(OAc) ₂		8		95

^aReaction conditions: Aryl halide (0.50 mmol), 4-methylphenylboronic acid (0.75 mmol), K₂CO₃ (1.5 mmol), H₂O (4.0 mL), and a catalyst containing Pd (0.054 mmol) at 80 °C. ^bTBAB (0.30 mmol) is added.

microfiltration and allowed the reaction to continue. The conversion stops increasing immediately (see Figure 8 and Supporting Information Figure S4). If a trace amount of soluble Pd species are the active species, the catalytic conversion should increase further, even after the removal of Pd/Y-MOF. (2) The coupling reaction is tested in the presence of poly(4-vinylpyridine),⁴² which is well-known as a solid poison to trap homogeneous Pd species in the solution phase through chelation. A comparison of conversion in C–C coupling reactions clearly demonstrates that the catalytic efficacy of Pd/Y-MOF is not affected when the PVPy is added to the reaction mixture (see Figure 8 and Supporting Information Figure S4), suggesting the reaction is only catalyzed by the solid Pd/Y-MOF. (3) The

three-phase test is considered a definitive test for answering the homogeneity/heterogeneity question. If leaching of active Pd species occurs, the supported reactant will undergo the same chemical reaction as the reactant present in the liquid medium. However, in the current case, the only product obtained in this process is derived from the reactant (iodobenzene) in the liquid phase. The supported reactant, 4-iodoacetophenone, which is immersed in the reaction solution but not directly contact with the solid catalyst remains unreacted, demonstrating that both the Suzuki–Miyaura and the Sonogashira coupling reaction are heterogeneous. (4) Microporous Pd/Y-MOF catalyst exhibits much higher activity for small-sized substrates than the bulky molecular species. If the reactions are

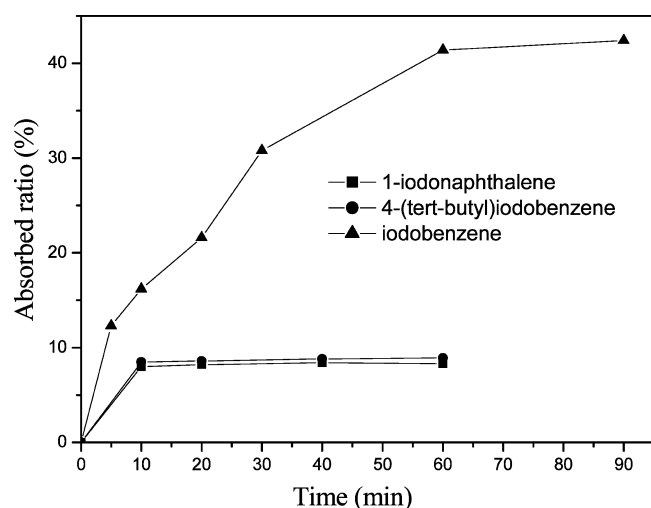


Figure 6. Adsorption test of Pd/Y-MOF catalyst for iodobenzene, 1-iodonaphthalene, and 4-(*tert*-butyl) iodobenzene.

catalyzed by dissolved Pd species, such size-selectivity will be very difficult to explain.

XPS analysis in Figure 9 shows almost identical patterns of Pd(II) in Pd/Y-MOF before and after the Suzuki coupling

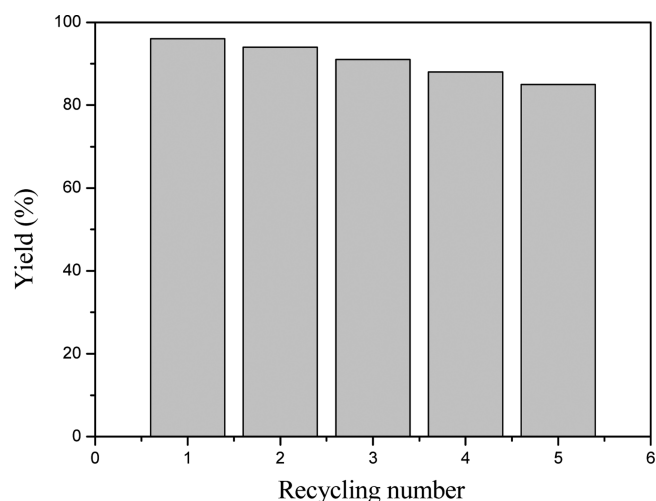


Figure 7. Durability test of Pd/Y-MOF catalyst in Suzuki–Miyaura coupling of iodobenzene and 4-methylphenylboronic acid. Reaction conditions are given in Table 3.

reaction. No peaks corresponding to Pd(0) in the metallic state is detected. The slight negative shifts and broadening of the Pd BE is ascribed to the oxidative addition of iodobenzene to Pd(II) on the surface and the formation of intermediate ArPdI.³²

Table 4. Sonogashira Reactions of Aryl Iodide with Arylacetylene^a

Catalyst	Recycling number	R	X	Reaction time (h)	Product	Yields (%)
Pd/Y-MOF	1	H	H	6		92
Pd/Y-MOF	2	H	H	6		90
Pd/Y-MOF	3	H	H	6		87
Pd/Y-MOF	1	CH ₃	H	6		82
Pd/Y-MOF	1	CH ₃ O	H	6		84
Pd/Y-MOF	1	NO ₂	H	4		99
Pd/Y-MOF	1	H	CH ₃ O	6		98
Pd/Y-MOF	1	H	F	6		79
Pd/Y-MOF	1	<i>t</i> -bu	H	6		7.5
Pd(bpydc)Cl ₂	1	H	H	6		61

^aReaction conditions: iodobenzene or substituted iodobenzene (0.50 mmol), phenylacetylene or substituted phenylacetylene (0.60 mmol), 1,8-diazabicyclo[5.4.0]undec-7-ene (DBU, 0.10 mL), H₂O (4.0 mL), *n*-decane (0.10 mL), and a catalyst containing Pd (0.054 mmol) at 90 °C.

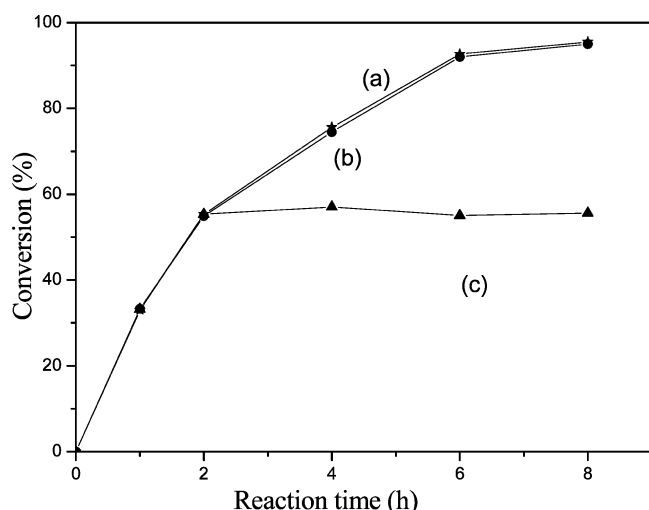


Figure 8. Plot of iodobenzene conversion of Suzuki–Miyaura coupling reactions, reaction conditions are given in Table 3. (a) Pd/Y-MOF activity without any poison; (b) adding PVPy as a poison at start of reaction; (c) removal of Pd/Y-MOF catalyst after 2 h reaction.

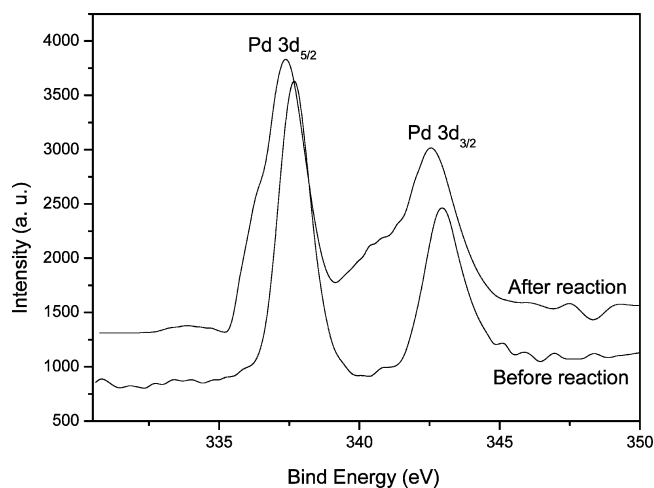


Figure 9. XPS spectra of Pd/Y-MOF before and after Suzuki–Miyaura coupling reaction.

There have been numerous works indicating that the coupling reactions occurred on the surface of the heterogeneous catalysts.^{32,39,49,50} In cases where Pd(II) is used, in situ reduction to Pd(0) is known to occur during the reaction, and the Pd(0) is catalytically active species. On the basis of the above heterogeneity studies, a plausible mechanism is proposed that the Suzuki–Miyaura and Sonogashira coupling reaction proceed in heterogeneous phase. The Pd(II) of Pd/Y-MOF in the coupling reaction seems to undergo a reversible process, in which Pd(II) is reduced to Pd(0) and immediately oxidized back to the initial Pd(II) state in situ when the reaction is carried out under the air atmosphere. The coordination of Pd–N and the stable Pd/Y-MOF frameworks prevent the formation of Pd(0) nanoparticles and the agglomeration of Pd(0) species into large Pd nanoparticles or Pd black.

CONCLUSIONS

We have synthesized a novel heterobimetallic Pd/Y-MOF catalyst through a facile microwave irradiation method. The 3D extended framework is constructed by Y(III) coordinating to

carboxylic groups on the Pd(bpydc)Cl₂ building blocks. For the small-sized reactant molecules, the catalytic activity of Pd/Y-MOF is comparable to Pd(OAc)₂ homogeneous catalyst owing to the high dispersion and accessibility of Pd(II) active sites in the layered structure and the cooperative effect of Y(III) coordination. Besides the high activity and size selectivity, Pd/Y-MOF can be easily recycled and reused owing to the excellent stability of MOF framework derived from the strong interaction of Y(III) and carboxyl. The coordination of Pd(II) and N atoms on bpydc prevented the leaching of Pd(II) active species under reaction conditions. Hot filtration test, solid-phase poisoning test, three-phase test and XPS analysis demonstrate that the catalytic nature of Pd/Y-MOF is heterogeneous. These studies indicate that the strategy can be served as a general method for the development of MOFs-based heterogeneous catalysts by fabrication of homogeneous counterparts into MOFs frameworks for practical catalytic applications.

ASSOCIATED CONTENT

Supporting Information

Detailed Rietveld structure refinement, Raman, and FT-IR spectra of the Pd/Y-MOF, the reaction process of Suzuki–Miyaura and Sonogashira, and the XRD patterns of the Pd/Y-MOF catalyst after being used repetitively in Sonogashira coupling reaction. This information is available free of charge via the Internet at <http://pubs.acs.org>.

AUTHOR INFORMATION

Corresponding Author

*E-mail: Hexing-Li@shnu.edu.cn (H.L.); wwang@unm.edu (W.W.).

Notes

The authors declare no competing financial interest.

ACKNOWLEDGMENTS

This work is supported by the National Natural Science Foundation of China (20825724) and Shanghai Government (10dj1400100).

REFERENCES

- (1) Férey, G.; Mellot, D. C.; Serre, C.; Millange, F.; Dutour, J.; Surblé, S.; Margiolaki, I. *Science* **2005**, *309*, 2040.
- (2) Banerjee, R.; Phan, A.; Wang, B.; Knobler, C.; Furukawa, H.; O’Keeffe, M.; Yaghi, O. M. *Science* **2008**, *319*, 939.
- (3) Corma, A.; Garcia, H.; Llabrés Xamena, F. X. *Chem. Rev.* **2010**, *110*, 4606.
- (4) Wang, Z.; Chen, G.; Ding, K. *Chem. Rev.* **2008**, *109*, 322.
- (5) Dinca, M.; Long, J. R. *J. Am. Chem. Soc.* **2005**, *127*, 9376.
- (6) Chen, B.; Ockwig, N. W.; Millward, A. R.; Contreras, D. S.; Yaghi, O. M. *Angew. Chem., Int. Ed.* **2005**, *44*, 4745.
- (7) Li, J.; Sculley, J.; Zhou, H. *Chem. Rev.* **2012**, *112*, 869.
- (8) Rybak, J.; Höller, C. J.; Matthes, P.; Müller, B. K.; Mai, M.; Feldmann, C.; Köhn, R.; Bein, T. *Z. Anorg. Allg. Chem.* **2010**, 2099.
- (9) Rocca, O. D.; Liu, D.; Lin, W. *Acc. Chem. Res.* **2011**, *44*, 957.
- (10) Kent, C. A.; Liu, D.; Ma, L.; Papanikolas, J. M.; Meyer, T. J.; Lin, W. *J. Am. Chem. Soc.* **2011**, *133*, 12940.
- (11) Pan, Y.; Yuan, B.; Li, Y.; He, D. *Chem. Commun.* **2010**, *46*, 2280.
- (12) Falkowski, J. M.; Wang, C.; Liu, S.; Lin, W. *Angew. Chem.* **2011**, *123*, 8833.
- (13) Lee, D.; Kim, J.; Jun, B.; Kang, H.; Park, J.; Lee, Y. *Org. Lett.* **2008**, *10*, 1609.
- (14) Schweizer, S.; Becht, J.; Le Drian, C. *Org. Lett.* **2007**, *9*, 3777.
- (15) Zhang, X.; Llabrés i Xamena, F. X.; Corma, A. *J. Catal.* **2009**, *265*, 155.

- (16) Llabrés i Xamena, F. X.; Abad, A.; Corma, A.; Garcia, H. J. *Catal.* **2007**, *250*, 294.
- (17) Tanabe, K. K.; Cohen, S. M. *Angew. Chem., Int. Ed.* **2009**, *121*, 756.
- (18) Saha, D.; Sen, R.; Maity, T.; Koner, S. *Langmuir* **2013**, *29*, 3140.
- (19) Lee, J.; Farha, O. K.; Roberts, J.; Scheidt, K. A.; Nguyen, S. T.; Hupp, J. T. *Chem. Soc. Rev.* **2009**, *38*, 1450.
- (20) Henschel, A.; Gedrich, K.; Kraehnert, R.; Kaskel, S. *Chem. Commun.* **2008**, 4192.
- (21) Martin, R.; Buchwald, S. L. *Acc. Chem. Res.* **2008**, *41*, 1461.
- (22) Polshettiwar, V.; Len, C.; Fihri, A. *Chem. Rev.* **2009**, *253*, 2599.
- (23) Yang, X.; Zhu, F.; Huang, J.; Zhang, F.; Li, H. *Chem. Mater.* **2009**, *21*, 4925.
- (24) Zhang, F.; Liu, G.; He, W.; Hong, Y.; Yang, X.; Li, H.; Zhu, J.; Li, H.; Lu, Y. *Adv. Funct. Mater.* **2008**, *18*, 3590.
- (25) Szeto, K. C.; Lillerud, K. P.; Tilset, M.; Bjørgen, M.; Prestipino, C.; Zecchina, A.; Lamberti, C.; Bordiga, S. *J. Phys. Chem. B* **2006**, *110*, 21509.
- (26) Szeto, K. C.; Prestipino, C.; Lamberti, C.; Zecchina, A.; Bordiga, S.; Bjørgen, M.; Tilset, M.; Lillerud, K. P. *Chem. Mater.* **2006**, *19*, 211.
- (27) Szeto, K. C.; Kongshaug, K. O.; Jakobsen, S.; Tilset, M.; Lillerud, K. P. *Dalton Trans.* **2008**, 2054.
- (28) Yin, L. X.; Liebscher, J. *Chem. Rev.* **2006**, *107*, 133.
- (29) Larson, A. C.; Von Dreele, R. B. *Los Alamos National Laboratory Report LAUR*; Los Alamos National Laboratory: Los Alamos, NM, 2004; pp 86–748.
- (30) Spek, A. L., *PLATON, A Multipurpose Crystallographic Tool*; Utrecht University: Utrecht, the Netherlands, 2001.
- (31) Yuan, B.; Pan, Y.; Li, Y.; Yin, B.; Jiang, H. *Angew. Chem., Int. Ed.* **2010**, *49*, 4054.
- (32) Choudary, B. M.; Madhi, S.; Chowdari, N. S.; Kantam, M. L.; Sreedhar, B. *J. Am. Chem. Soc.* **2002**, *124*, 14127.
- (33) Koner, S.; Ghosh, A.; Chaudhuri, N. R.; Mukherjee, M. *Polyhedron* **1993**, *12*, 2551.
- (34) Thomas, A. C. *Photoelectron and Auger Spectroscopy*; Plenum: New York, 1975.
- (35) Reineke, T. M.; Eddaoudi, M.; O'Keeffe, M.; Yaghi, O. M. *Angew. Chem., Int. Ed.* **1999**, *38*, 2590.
- (36) Anja, C. F.; Matthias, B. *Angew. Chem., Int. Ed.* **2005**, *44*, 674.
- (37) Comins, D. L.; Dehghani, A. *Tetrahedron Lett.* **1992**, *33*, 6299.
- (38) Hartwig, J. F.; Richards, S.; Baranano, D.; Paul, F. *J. Am. Chem. Soc.* **1996**, *118*, 3626.
- (39) Minkee, C.; Dong-Hwan, L.; Kyungsu, N.; Byung-Woo, Y.; Ryong, R. *Angew. Chem., Int. Ed.* **2009**, *48*, 3673.
- (40) Molnar, A. *Chem. Rev.* **2011**, *111*, 2251.
- (41) Choi, M.; Lee, D. H.; Na, K.; Yu, B. W.; Ryoo, R. *Angew. Chem., Int. Ed.* **2009**, *48*, 3673.
- (42) Ji, Y.; Jain, S.; Davis, R. J. *J. Phys. Chem. B* **2005**, *109*, 17232.
- (43) Richardson, J. M.; Jones, C. W. *Adv. Synth. Catal.* **2006**, *348*, 1207.
- (44) Jana, S.; Haldar, S.; Koner, S. *Tetrahedron Lett.* **2009**, *50*, 4820.
- (45) Jana, S.; Dutta, B.; Bera, R.; Koner, S. *Inorg. Chem.* **2008**, *47*, 5512.
- (46) Richardson, J.; Jones, C. *J. Catal.* **2007**, *251*, 80.
- (47) Das, D.; Sayari, A. *J. Catal.* **2007**, *246*, 60.
- (48) Rebek, J.; Gavina, F. *J. Am. Chem. Soc.* **1974**, *96*, 7112.
- (49) Ellis, P. J.; Fairlamb, I. J.; Hackett, S. F.; Wilson, K.; Lee, A. F. *Angew. Chem., Int. Ed.* **2010**, *49*, 1820.
- (50) Augustine, R. L.; O'Leary, S. T. *J. Mol. Catal. A: Chem.* **1995**, *95*, 277.